Published in final edited form as:
Sci Signal. 2017 January 10; 10(461): . doi:10.1126/scisignal.aah4874.

Synergistic regulation of serotonin and opioid signaling contribute to pain insensitivity in $Na_v1.7$ knockout mice

Jörg Isensee[1,*], **Leonhardt Krahé**[1], **Katharina Moeller**[1], **Vanessa Pereira**[2], **Jane E. Sexton**[2], **Xiaohui Sun**[2], **Edward Emery**[2], **John N. Wood**[2], **Tim Hucho**[1,*]

[1]Department of Anesthesiology and Intensive Care Medicine, Experimental Anesthesiology and Pain Research, University Hospital of Cologne, Robert Koch Str. 10, 50931 Cologne, Germany

[2]Molecular Nociception Group, WIBR, University College London, Gower Street, London WC1E 6BT, UK

Abstract

Genetic loss of the voltage-gated sodium channel $Na_v1.7$ ($Nav1.7^{-/-}$) results in lifelong insensitivity to pain in mice and humans. One underlying cause is an increase in the production of endogenous opioids in sensory neurons. We analyzed whether $Na_v1.7$ deficiency altered nociceptive heterotrimeric guanine nucleotide–binding protein–coupled receptor (GPCR) signaling, such as initiated by GPCRs that respond to serotonin (pronociceptive) or opioids (antinociceptive), in sensory neurons. We found that the nociceptive neurons of $Na_v1.7$ knockout ($Na_v1.7^{-/-}$) mice, but not of $Na_v1.8$ knockout ($Na_v1.8^{-/-}$) mice, exhibited decreased pro-nociceptive serotonergic signaling through the $5\text{-}HT_4$ receptors, which are Gαs-coupled GPCRs that stimulate the production of cyclic adenosine monophosphate resulting in protein kinase A (PKA) activity, as well as reduced abundance of the RIIβ regulatory subunit of PKA. Simultaneously, the efficacy of anti-nociceptive opioid signaling mediated by the $G\alpha_i$-coupled mu opioid receptor was increased. Consequently, opioids inhibited more efficiently tetrodotoxin-resistant sodium currents, which are important for pain-initiating neuronal activity in nociceptive neurons. Thus, $Na_v1.7$ controls the efficacy and balance of GPCR mediated pro- and antinociceptive intracellular signaling, such that without $Na_v1.7$, the balance is shifted toward antinociception, resulting in lifelong endogenous analgesia.

Introduction

Novel strategies to treat pain are urgently required; more than 20% of patients do not respond to current analgesics (1, 2). In addition, even for the responding patients, the therapeutic efficacy of opioid treatment requires improvement. Opioids, which are considered benchmark analgesics, decrease the individual pain rating in average by only

*For material and correspondence, please contact J.I. (joerg.isensee@uk-koeln.de) and T.H. (tim.hucho@uk-koeln.de).

Author contributions: J.I. and T.H. designed the study and wrote the manuscript. J.I., L.K., K.M. performed cellular experiments. V.P. produced transgenic mice and performed qPCR assays. J.S. contributed to experimental design and data analysis of the electrophysiological experiments. J.N.W. supplied and helped analyze transgenic mice. E.E., X.S. designed and performed electrophysiological experiments and analysed data. J.N.W., V.P., J.S., E.E. contributed to writing the manuscript.

Competing interests: There are no competing financial interests to declare.

Europe PMC Funders Author Manuscripts

10-15% (3–5). Additionally, opioid treatment bears the risk of addiction and the potential for life-threatening side effects (6,7). These adverse effects are aggravated because patients receiving opioids quickly desensitize and therefore require ever-increasing doses. Furthermore, currently, desensitization due to the prolonged use of opioids can only be reduced but not abolished (8).

Voltage-gated sodium channels, such as $Na_v1.7$, are central for the sensitivity and activation of nociceptive neurons in response to pain-initiating stimuli. Although otherwise apparently normal, loss of function of $Na_v1.7$ results in lifelong absence of pain (congenital insensitivity to pain) in mice and humans without loss of the nociceptive neurons or their ability to fire action potentials (9–11). The central role of $Na_v1.7$ in pain and its presence predominantly in nociceptive neurons make it an excellent potential target for analgesic drug development (12, 13). Nevertheless, potent $Na_v1.7$ blockers fail to alleviate pain (14).

The exact mechanisms responsible for pain insensitivity due to loss of $Na_v1.7$ are incompletely understood (12). $Na_v1.7$-deficiency ($Na_v1.7^{-/-}$) results in increased expression of the gene encoding the endogenous opioid met-enkephalin and increased met-enkephalin immunoreactivity in sensory neurons (15). In addition, blocking opioid receptors with naloxone restores the ability to perceive pain in mice and humans (15), consistent with these neurons being electrically functional, yet inappropriately responsive. These data indicate that, in addition to its role in electrical signaling, $Na_v1.7$ is likely to have other functions that contribute to pain sensitivity. Whether the absence of $Na_v1.7$ only affects the abundance of endogenous opioids or whether intracellular pain signaling is also altered remains unknown.

Whereas opioid signaling is anti-nociceptive (inhibits pain signaling), 5-HT is a pronociceptive (promotes pain signaling).

In addition to increased expression of the gene encoding endogenous opioids, gene expression profiling in dorsal root ganglia of Nav1.7-deficient mice identified reduced transcripts encoding the metabotropic serotonin (5-HT) receptor $5\text{-}HT_4$ (15), suggesting that the absence of $Na_v1.7$ may change not only antinociceptive but also pronociceptive signaling in sensory neurons.

We investigated whether the absence of $Na_v1.7$ reduced $5\text{-}HT_4$ receptor-mediated pro-nociceptive signaling, whether the opioid signaling is altered beyond the described increase of met-enkephalin, and whether the changes of the pro- and antinociceptive intracellular signaling occur synergistically in the same sensory neurons.

Both $G\alpha_s$- and $G\alpha_i$-coupled GPCRs converge on adenylyl cyclase, such that Gαs-coupled receptors such as the $5\text{-}HT_4$ receptor (16–17) promote cAMP production and PKA signaling and $G\alpha_i$-coupled receptors such as the mu opioid receptor (MOR) (18) inhibit this pathway. We used an assay for changes of cyclic adenosine monophosphate (cAMP)–induced protein kinase A (PKA) activity in untransfected primary sensory neurons (19). Thus, with this assay, we could monitor GPCR-mediated pro- and antinociceptive signaling and the balance between these two inputs in individual neurons. To discern specific effects of the absence of $Na_v1.7$, we compared neurons from $Na_v1.7$-deficient mice with neurons from wild-type and $Na_v1.8$-deficient ($Na_v1.8^{-/-}$) mice. $Na_v1.8^{-/-}$ mice exhibit a different pain-deficient

phenotype. $Na_v1.8$-deficient mice have a pronounced analgesia to noxious mechanical stimuli, small deficits in noxious thermoreception, and delayed development of inflammatory hyperalgesia (20). These mice served as a control to show the specificity of the mechanism by which loss of $Na_v1.7$ produces congenital insensitivity to pain.

Single-cell analysis of primary neurons from wild-type, $Na_v1.7$-deficient, and $Na_v1.8$-deficient mice revealed that the absence of $Na_v1.7$ but not of $Na_v1.8$ resulted in decreased responsiveness to 5-HT and increased opioid receptor signaling. Both changes occurred synergistically in the same cells, resulting in enhanced efficacy of opioid signaling for reducing currents through the class of tetrodotoxin-resistant (TTXr) voltage-gated sodium channels, which is particularly important for action potential generation in nociceptive neurons (12). Thus, $Na_v1.7$, which are also tetrodotoxin-sensitive voltage-gated sodium channels, appear to control the homeostatic set point for pro- and anti-nociceptive intracellular signaling in sensory neurons.

Results

The 5-HT_4 receptor is critical for the activation of PKA-II in sensory neurons from dorsal root ganglia

Pronociceptive metabotropic serotonin receptors stimulate the activity of PKA; antinociceptive opioid receptors inhibit PKA activity. To test for differences in the balance of these two inputs, we first identified which $G\alpha_s$-coupled metabotropic serotonin receptor, 5-HT_4, 5-HT_6, or 5-HT_7, had the strongest influence on PKA signaling in individual sensory neurons, a question that has been controversial for long (17, 21, 22). PKA signaling is activated by cAMP resulting in dissociation of catalytic subunits from inhibitory sites of the PKA-II regulatory subunits RIIα and RIIβ (collectively referred to as pRII), which increases the relative binding of phosphorylation-specific antibodies against RII sites (19). Inactivation of PKA-II requires degradation of cAMP by phosphodiesterases and dephosphorylation of RII subunits before reassociation of catalytic and regulatory subunits (23). To evaluate the relative amount of PKA signaling in single neurons, we used a “High Content Screening (HCS)” microscopy approach to detect pRII in primary neurons isolated from dorsal root ganglia from adult male rats (19, 24). This assay relies on signals from fluorescently tagged antibodies that distinguish neurons on the basis of the presence of the neuronal marker ubiquitin C-terminal hydrolase L1 (UCHL1) and nociceptive sensory neurons on the basis of the presence of RIIβ, and quantifies the activity of cAMP-activated PKA by detecting pRII with antibodies that recognize the phosphorylated forms of both RIIα and RIIβ (Fig. 1A and fig. S1).

Because $Na_v1.7$-deficient mice had reduced transcripts encoding the metabotropic serotonin receptor 5-HT_4 (15), we tested the effect of 5-HT, the 5-HT_4-specific agonist SC-53116 (25) and the 5-HT_4-specific antagonist GR113808 (26) in the cultured neurons on pRII. Both 5-HT and SC-53116 increased the intensity of the pRII signal with similar potency in rat sensory neurons (Fig. 1B). GR113808 blocked the 5-HT-induced increase in pRII (Fig. 1C). The 5-HT_4 agonist and antagonist results indicated that this serotonin receptor is both sufficient and necessary for 5-HT-induced increase in pRII in sensory neurons. Thus, our

results suggested that the reported reduction in 5-HT_4 receptor-encoding mRNA in $Na_v1.7^{-/-}$ (15) may result in a reduction of this pro-nociceptive signaling pathway in sensory neurons.

Opioids inhibit the 5-HT-induced PKA-II activation

To examine if the increase in production of opioids attenuated 5-HT signaling in individual sensory neurons, we used the pRII HCS microscopy assay to examine the response to opioids of neurons exposed to 5-HT. We stimulated the neurons with 5-HT, which increased the detected immune-pRII intensity, and then added increasing concentrations of opioid receptor ligands and monitored the effect on pRII signals. The clinically relevant opioid analgesic fentanyl and the MOR-specific agonist DAMGO dose dependently inhibited the 5-HT-induced pRII signal in rat sensory neurons (Fig. 1D), with fentanyl being the more potent of the two. Coapplication of fentanyl with 5-HT produced long-lasting inhibition of 5-HT responses at all tested doses, but fentanyl did not affect basal pRII intensity when applied alone, indicating these neurons already had low basal adenylyl cyclase activity and thus low PKA-II activity (Fig. 1E). The competitive opioid receptor antagonist naltrexone reversed the fentanyl-induced inhibition of pRII intensity (Fig. 1F). Naltrexone alone had no effect on basal or 5-HT-induced pRII intensity (Fig. 1G), indicating the absence of basal opioid receptor activity in cultured rat sensory neurons. The MOR-specific antagonist CTOP did not affect basal or 5-HT induced pRII intensity and only partially blocked the fentanyl-induced inhibition of pRII (Fig. 1, H and I). Coapplication of DAMGO with 5-HT also resulted in a dose-dependent, sustained inhibition of the 5-HT-induced increase in pRII (Fig. 1J), which was fully reversed by naltrexone (Fig. 1L) and partially by CTOP (Fig. 1L). The ability of opioids to inhibit PKA-II activity was not limited to that stimulated by 5-HT, but also extended to PKA-II activity induced by the IP_1 receptor agonist prostacyclin (PGI_2) or the adenylyl cyclase activator forskolin (Fsk) (fig. S2).

We identified RIIβ as a marker of nociceptive subgroups (19). According to transcriptome data (27), the gene encoding RIIβ should be coexpressed with the gene encoding the opioid receptors. To demonstrate the sensitivity of RIIβ(+) neurons to opioids, we analyzed the effect of fentanyl on the response to Fsk, 5-HT, or PGI_2 in RIIβ-negative and RIIβ-positive sensory neurons (Fig. 2A). After compensating for potential spill-over between fluorescence channels (Fig. 2B), we found that Fsk increased the pRII intensity in all rat sensory neurons, both RIIβ(-) and RIIβ(+) neurons; whereas 5-HT and PGI_2 predominately activated RIIβ(+) neurons (Fig. 2A, C, D). Furthermore, we found that inhibitory effect of fentanyl on Fsk-induced pRII was restricted to the RIIβ(+) subgroup (Fig. 2A and C), indicating that RIIβ is an indicator of sensitivity to opioids.

5-HT signaling is reduced in $Na_v1.7^{-/-}$ mice

With the results from wild-type rat dorsal root ganglia neurons, we could investigate if loss of $Na_v1.7$ results in long-lasting changes in nociceptive neurons in addition to the reported increase in *PENK* expression (the gene encoding endogenous opioid precursors) in dorsal root ganglia and the processed opioid ligand met-enkephalin in the dorsal horn of the spinal cord (15). We analyzed pRII as an indicator of functional PKA-II activation in pain-insensitive $Na_v1.7^{-/-}$ mice (10). $Na_v1.8^{-/-}$ mice served as a control for animals lacking a related voltage-gated Na^+ channel. These mice have a pain-insensitivity phenotype that is

different from and less severe than that of the Nav1.7$^{-/-}$ mice (20). We assessed general features of the cultures of dissociated dorsal root ganglia from mice of both genotypes (Fig 3A). Overall numbers of cells and the cell size distribution and intensity distribution of the neuronal marker UCHL1 were highly similar, indicating comparability among the genotypes (Fig. 3B). Using quantitative reverse transcriptase polymerase chain reaction (qRT-PCR), we confirmed that *Hrt4* transcript abundance was reduced in sensory ganglia of $Na_v1.7^{-/-}$ mice and not $Na_v1.8^{-/-}$ mice (Fig. 3C). The results with the $Na_v1.7^{-/-}$ mice are consistent with the microarray data by Minett *et al.* (15).

To test for functional cellular changes associated with absence of $Na_v1.7$ and reduced expression of the gene encoding 5-HT_4 for PKA-II signaling, we compared the responses of dorsal root ganglia cells isolated from wild-type $Na_v1.7^{+/+}$ and $Na_v1.7^{-/-}$ mice using the pRII assay. We tested the response to different GPCR ligands (5-HT, PGI_2), to the adenylyl cyclase activator Fsk, and to the cell-permeable cAMP analog Sp-8-Br-cAMPS-AM (8-bromoadenosine-3′,5′-cyclic monophosphorothioate, Sp-isomer, and acetoxymethyl ester). Costaining for pRII and RIIβ revealed that $Na_v1.7$ deficiency results in reduced numbers of cells that respond to 5-HT (Fig. 3D). Consistent with the reduced *Hrt4* transcript abundance leading to less receptor, the maximum amplitude but not the EC_{50} of the pRII response to 5-HT was reduced in sensory neurons of $Na_v1.7^{-/-}$ mice (Fig. 3E). pRII responses to PGI_2, Fsk, or Sp-8-Br-cAMPS-AM were the same in cultures from the $Na_v1.7^{+/+}$ and $Na_v1.7^{-/-}$ mice (Fig. 3E).

The similarity in the dose responses of the downstream activators Fsk and Sp-8-Br-cAMPS-AM between $Na_v1.7^{+/+}$ and $Na_v1.7^{-/-}$ mice (Fig. 3G) indicated that the reduction in response to 5-HT resulted from a change at the receptor level and not of downstream effectors such as adenylyl cyclases. The similarity in the responses of neurons to PGI_2 in both genotypes indicated that the general ability to signal through Gαs-coupled GPCRs was not impaired but that the reduced pRII response was specific for 5-HT stimulation of 5-HT_4 receptors (Fig. 3G). These data confirmed that sensory neurons from animals deficient in either of these two voltage-gated Na^+ channels were functional with regard to their ability to activate PKA signaling and that only mice deficient for $Na_v1.7$ exhibited reduced *Hrt4*.

RIIβ is less abundant in dorsal root ganglia from $Na_v1.7^{-/-}$ mice

The pRII dose response data presented in Fig. 3E were normalized. However, analysis of the non-normalized data as presented in the kinetic experiments revealed an additional reduction of pRII baseline intensity values by 8% in $Na_v1.7^{-/-}$ mice compared to wild-type litters (Fig. 4A, Ctrl). This was unexpected, because the baseline activity of PKA-II is commonly tightly controlled and maintained at a constant level (28, 29). Thus, the observed reduction in baseline activity indicates that $Na_v1.7$ deficiency resulted in another change that could affect intracellular signaling. Similar to the reduction in 5-HT_4 receptors, this effect on the basal amount of pRII was specific for $Na_v1.7^{-/-}$ mice and not present in $Na_v1.8^{-/-}$ mice (Fig. 4B, Ctrl). A reduced pRII signal could be the result of the identified downregulation of 5-HT_4-mediated input. However, we observed that also the phosphorylation signals in response to Fsk were also lower than those in wild-type (Fig. 4A, Fsk). This effect was specific to

$Na_v1.7^{-/-}$ mice because we did not detect this reduction in pRII intensity in $Na_v1.8^{-/-}$ mice (Fig. 4B, Fsk).

The reduction in the amount of pRII could result from reduced abundance of total RII because of reduced gene expression or increased degradation or could result from reduced phosphorylation. Therefore, we analyzed for the abundance of RIIβ, the major PKA-RII regulatory subunit in rat nociceptive neurons (19). As in rats, we also found that in mice, RIIβ was enriched in small-to-medium sized sensory neurons (Fig. 4C). $Na_v1.7$ deficiency did not affect the number of RIIβ(+) neurons, but resulted in a general shift towards lower RIIβ intensities (Fig. 4C and D). The mean RIIβ intensity was 11% lower in RIIβ(+) neurons of $Na_v1.7^{-/-}$ mice compared to that in neurons from wild-type litters (Fig. 4E). These data indicate that the 5-HT pronociceptive input and the mediating intracellular signaling component RIIβ are reduced in $Na_v1.7^{-/-}$ mice.

Opioid signaling is amplified in $Na_v1.7^{-/-}$ mice

We next investigated the effect of $Na_v1.7$ or $Na_v1.8$ deficiency on the cellular activity of the anti-nociceptive opioid receptor signaling system using the nonspecific opioid receptor agonist fentanyl and the nonspecific antagonist naltrexone. Neither fentanyl nor naltrexone altered the baseline amount of pRII in neurons from $Na_v1.7^{-/-}$ or $Na_v1.8^{-/-}$ mice (Fig. 4A and B, Fent and NTX). These results are consistent with those we obtained for wild-type rat pain-sensing neurons (Fig. 1F and G). The absence of an effect of naltrexone indicated that there is no basal opioid receptor activity in the neurons from the $Na_v1.7^{-/-}$ mice or wild-type rat pain-sensing neurons. The lack of an effect of fentanyl indicated that the basal adenylyl cyclase activity and thus PKA activity and pRII abundance were low in the cells under basal conditions and activation of the opioid receptor did not further suppress this pathway.

Next, we tested the effect of fentanyl and naltrexone on changes of pRII intensity induced by 5-HT. The $Na_v1.7^{-/-}$ mice have increased production of endogenous opioids(15), which would be expected to result in opioid receptor desensitization because of prolonged opioid exposure (30). However, we found that the inhibition of the 5-HT-induced pRII intensity by fentanyl was greater in sensory neurons of $Na_v1.7^{-/-}$ mice compared with the inhibitory effect in neurons from the wild-type mice. (Fig. 4A, 5-HT/Fent). The response to 5-HT was less in the neurons from the $Na_v1.7^{-/-}$ mice (Fig. 4A, 5-HT), consistent with the downregulation of $5\text{-}HT_4$ receptors; however, fentanyl completely abolished the 5-HT response in the neurons from the $Na_v1.7^{-/-}$ mice (Fig. 4A, 5-HT/Fent). This fentanyl effect was mediated by opioid receptors, because naltrexone antagonized the fentanyl effect (Fig. 4A, 5-HT/Fent/NTX). This phenotype was absent in $Na_v1.8^{-/-}$ mice (Fig. 4B, 5-HT, 5-HT/Fent, 5-HT/Fent/NTX), suggesting a specific role for $Na_v1.7$ in regulating opioid receptor signaling.

To analyze how these differences in responses distributed over subgroups of sensory neurons, we plotted the pRII intensities of all analyzed neurons versus their size and applied fixed intensity and size thresholds to evaluate the number of responding neurons (Fig. 4F). We compared the percent of small-sized sensory neurons that exceeded the threshold for pRII intensity of neurons from wild-type and $Na_v1.7^{-/-}$ mice. We compared the population size in control conditions, in response to individual exposure to anti-nociceptive or pro-

nociceptive agonists and to their combination. Stimulation with 5-HT increased pRII signals in 17% of smaller sized sensory neurons from $Na_v1.7^{-/-}$ mice and in 21% from wild-type mice. Simultaneous application of fentanyl reduced the number of 5-HT-responsive neurons from 17% to 6% in $Na_v1.7^{-/-}$ (Fig. 4F, red arrow) and from 21% to 17% in wildtypes (Fig. 4F, 5-HT/Fent). Thus, the signaling amplitude (Fig. 4A) and the number of cells responding to 5-HT in the presence of fentanyl was reduced in $Na_v1.7^{-/-}$ animals (Fig. 4F).

Coincident activation of stimulatory and inhibitory GPCRs is considered to augment the sensitivity, amplitude and duration of G_i signaling by a mechanism involving cAMP-dependent interaction of RII subunits with Gαi proteins (31). Thus, a reduced 5-HT pro-nociceptive input should result in a reduced anti-nociceptive opioid-input. The relative opioid inhibition should remain the same.

We compared the pRII response of neurons from wild-type or $Na_v1.7^{-/-}$ mice exposed to a single concentration of 5-HT and increasing concentrations of fentanyl to determine how the reduced 5-HT-mediated pronociceptive input affected the dose-response relationship for fentanyl (Fig. 5A and B). The IC_{50} values (16 nM for $Na_v1.7^{-/-}$ neurons and 36 nM for wild-type neurons) were not significantly different between the two genotypes, suggesting a similar receptor-ligand affinity. Nevertheless, the response amplitude of fentanyl over the entire dose-response curve was shifted to lower amplitudes in the $Na_v1.7^{-/-}$-deficient neurons (Fig. 5A). This shift was unexpected if the G_i response scales with the G_s input as has been reported (31). This effect was not merely because neurons from the $Na_v1.7$-deficient mice responded less to 5-HT but also to the relative effect of fentanyl on 5-HT responding neurons being higher in neurons from Nav1.7-deficient animals, indicating increased effectiveness of the opioid-mediated signal (fig. S3A). At the single cell level, the opioid response was shown to be a specific effect of the 5-HT-responding RIIβ(+) neurons (Fig. 5B). In addition, this effect was caused by fewer cells reacting and a larger percentage of responding cells being inhibited by fentanyl (fig. S3B). We obtained similar results with DAMGO: The IC_{50} to inhibit 5-HT-induced pRII was similar, but the maximum response was greater in neurons from the $Na_v1.7^{-/-}$ mice (fig. S3E and F).

To determine if the enhanced effectiveness of opioid signaling in the absence of $Na_v1.7$ was independent of the pRII-inducing receptor stimulus, we applied increasing doses of fentanyl in the presence of Fsk. The effectiveness of fentanyl was significantly enhanced in $Na_v1.7$-deficient neurons (Fig. 5C and fig. S3C). Consistent with the observed reduction in basal RIIβ and pRII signal (Fig. 4), single-cell analysis showed that the number of Fsk-stimulated neurons was significantly less in the $Na_v1.7$-deficient mice in the absence of fentanyl (Fig. 5D). Fentanyl reduced the population of responding cells by 39% in $Na_v1.7^{+/+}$ (28% at 0 μM to 17% at 2 μM fentanyl) while by 61% in $Na_v1.7^{-/-}$ mice (23% at 0 μM to 9% at 2 μM fentanyl) (Fig. 5D and fig. S3D). The increased inhibition of Fsk responsive neurons by fentanyl in Nav1.7-deficient neurons remained significant even after normalization to remove the effect of basal differences in the number of Fsk responsive neurons (fig. S3D). Thus, the relative as well as the absolute reduction by opioids of the pRII signal and the responding cell number was substantially enhanced in $Na_v1.7^{-/-}$.

Synergistic dampening of pain signaling renders opioids more effective in reducing sodium currents

One functional consequence of PKA signaling in pain-sensing neurons is enhanced activity of the $Na_v1.8$ channel and increased $Na_v1.8$-mediated current (32, 33). To determine whether the shift in the balance of pro- and anti-nociceptive signaling efficiency (reduced and increased, respectively) altered the ability of opioids to suppress TTXr sodium currents, we performed voltage-clamp analysis of in vitro cultured sensory neurons from wild-type and $Na_v1.7^{-/-}$ mice and measured TTXr sodium currents in the presence and absence of fentanyl (Fig. 6). After normalizing the baseline currents, we found that fentanyl produced a greater reduction in $Na_v1.8$ TTXr currents in the cells from the $Na_v1.7^{-/-}$ mice (Fig. 6B, C). These results are consistent with the cellular studies of showing that opioid signaling was more effective at reducing PKA activity in $Na_v1.7^{-/-}$ mice (Fig. 5). This enhanced opioid-mediated reduction in sodium current would make the neurons less active, which suggests that the altered pro- and anti-nociceptive signaling that we observed likely contributes to the analgesic phenotype of mouse and human $Na_v1.7^{-/-}$ mutants.

In conclusion, our data indicate that the absence of $Na_v1.7$ results in significantly reduced 5-HT pro-nociceptive input, with a concomitant reduction of the intracellular mediator RIIβ and the abundance of pRII. Concomitant with the reduction in pro-nociceptive signaling, anti-nociceptive input and signaling effectiveness was enhanced, resulting in a synergistic reduction in pain sensitivity and neuronal sodium current activity. Because these synergistic changes occurred specifically in the absence of $Na_v1.7$, but not of $Na_v1.8$, the balance of pro- versus anti-nociceptive signaling is controlled specifically by $Na_v1.7$.

Discussion

Genetic loss of function of $Na_v1.7$ causes congenital insensitivity to pain in mice and humans (9, 11, 34), yet acute block of $Na_v1.7$ with potent and selective $Na_v1.7$ antagonists does not (14). This contradiction could be resolved if $Na_v1.7$ contributes not only acutely to electrical activity but regulates also other cellular processes measurable after prolonged times of channel inhibition and/or by other readout parameters than acute analgesia. Beyond changes of acute electrical activity, Minett *et al.* found in the spinal cord of $Na_v1.7^{-/-}$ mice that also substance P release is abolished and opioid activity is tonically increased(10, 15). Both observations, nevertheless, may be the direct consequence of reduced depolarization and thereby reduced depolarization-induced secretion of vesicles containing substance P or opioid or both kinds of secretory vesicles. In contrast, here, we showed that animals lacking $Na_v1.7$ have alterations beyond the acute depolarization event. We found the loss of functional $Na_v1.7$ to result in prolonged altered pro- and anti-nociceptive GPCR signaling within sensory neurons even in the neutral environment of cell culture medium (Fig. 7).

Our results highlight the intimate interaction between pro- and anti-nociceptive inputs. 5-HT has been described as countering the effects of opioids on system level. For example, agonists of $5\text{-}HT_4$ receptors are used to counteract constipation resulting from chronic opioid use (35, 36) and to counteract opioid-induced respiratory depression (37). At the level of neuronal circuits, 5-HT-reuptake inhibitors counteract afferent pain-input by increasing the activity of descending inhibitory neurons in the spinal cord (38, 39). Our results further

support this antagonistic role: We found 5-HT_4 receptor signaling and opioid signaling were functionally connected at the single-cell level in a subgroup of peripheral nociceptive neurons.

The balance between pro- and anti-nociceptive input scales with stimulus intensity. Thus, increased pro-nociceptive input results in a concomitant increase in the counterbalancing opioid anti-nociceptive signal to maintain a constant net response (31). Our results indicate that, without $Na_v1.7$, this scaling does not occur (Fig. 7). We found that the reduction of the pro-nociceptive serotonergic input in $Na_v1.7^{-/-}$ is not followed by a corresponding reduction of the opioid input. On the contrary, the effectiveness of opioid signaling was significantly increased, resulting in stronger inhibition of pRII and suppression of TTXr sodium currents. Whereas about 50% of the serotonin-induced pRII pro-nociceptive signaling remained even after maximal doses of opioid treatment in neurons from wild-type animals, the serotonin-induced pRII pro-nociceptive signal was nearly completely abolished by maximal doses of opioids in $Na_v1.7^{-/-}$ neurons (Fig. 5A, B and fig. S3A, B). This increased efficacy could be of importance in respect to the only moderate effectiveness of opioids in patients, which is in average at 10-15% (3–5). Thus, it will be of importance to test if a pharmacological block of $Na_v1.7$ results in a similar increase in the cellular efficacy of opioids and if this also translates into increased pain reduction that exceeds the currently observed average of 10-15% pain relief in patients. Even further, desensitization to prolonged presence of opioids is the net result of opioid receptor internalization, receptor uncoupling, as well as of the upscaling of the counteracting pro-nociceptive signaling that we identified here. Thus, it will be of interest to detail if and how the lack of $Na_v1.7$ and the observed lack of scaling results in reduced opioid induced desensitization (8). It will be especially interesting to test if pharmacological inhibitors of $Na_v1.7$ result in a similar reduction of the scaling effect, which might have been missed in studies solely evaluating for acute $Na_v1.7$-inhibitor induced analgesia. A report about the increased effectiveness of opioids by combining them with the blocker of voltage gated sodium channels including $Na_v1.7$, lidocaine, could indicate such a pharmacologically induced synergism (40).

PENK mRNA is upregulated in the complete absence of $Na_v1.7$ activity but not after partial blockade (15). However, some GPCRs are also rapidly modulated by non-transcriptional changes that are initiated by changes in intracellular sodium concentration. Increased intracellular sodium concentration affects GPCR ligand binding and allosteric regulation of biased signaling. In particular, increased intracellular sodium uncouples opioid receptors from $G\alpha_i$ and increases the constitutive signaling activity through the β-arrestin pathway (41–44). A reduction in the intracellular concentration of sodium could explain the observed increased $G\alpha_i$ signaling activity resulting in the enhanced reduction of PKA activity. However, the specificity of our observations to $Na_v1.7^{-/-}$ but not to $Na_v1.8^{-/-}$ mice, which still have remaining nociceptive neuron activity and pain reception (20), argues against large changes in intracellular sodium concentration as the cause of the increase in opioid receptor signaling efficacy. Still, another possibility is that $Na_v1.7$ and opioid receptors could be colocalized in signaling hubs that enable local changes in sodium concentration to influence opioid receptor activity. Future work is needed to detail the mechanism leading to the synergistic changes that dampen pain signaling.

The loss of function of $Na_v1.7$ appears to cause long-term changes to intracellular nociceptive signaling, and we found these changes were present even in the absence of exogenously added opioids, which may indicate that the continuous presence of opioids is unnecessary to maintain the altered signaling state. Our finding of reduced pronociceptive input and increased effectiveness of antinociceptive opioids provides evidence that sustained dampening of the intracellular pain signaling in nociceptive neurons can be achieved, at least in the absence of $Na_v1.7$. Our results indicated that $Na_v1.7$ may regulate the homeostatic set point of pain signaling, which is in agreement with previous reports of the close link of the expression of the gene encoding $Na_v1.7$, its abundance, and pain (15, 31, 45, 46). We propose that our assay, which monitors pro- and antinociceptive signaling as well as RIIβ abundance in one single readout, can be used to identify potential drug candidates that shift the balance of these in favor of anti-nociceptive signaling. Current inhibitors of $Na_v1.7$ activity lack direct analgesic activity on their own. However, our data suggest the possibility that some pain conditions will benefit from opioid treatment combined with inhibition of $Na_v1.7$, which could prolong as well as enhance opioid effectiveness, thereby offering better pain management.

Materials & Methods

Antibodies

The following antibodies were used in this study: chicken polyclonal antibodies against UCHL1 (1:2000, Novus, Cambridge, UK, #NB110-58872), rabbit monoclonal antibody against phosphorylated RIIα (S96) (1:1000, clone 151, Abcam, Cambridge, UK, #ab32390), mouse monoclonal antibody against RIIβ (1:2000, BD Transduction Laboratories, #610625), highly cross-adsorbed Alexa 647, 594, and 488 conjugated secondary antibodies (Invitrogen, Carlsbad, CA).

Reagents

5-HT (10 mM in dH_2O), naltrexone (100 mM in dH2O), SC-53116 (100 mM in DMSO), GR113808 (100 mM in DMSO) were purchased from Sigma-Aldrich (Munich, Germany) and dissolved as indicated as stock solutions. Fentanyl (10 mM in dH_2O), DAMGO (10 mM in PBS, pH 7.4), CTOP (5 mM in DMSO), and fsk (10 mM in DMSO) were from Tocris (Bristol, UK). Prostacyclin (10 mM in PBS, pH9.5) was from Cayman (Ann Arbor, MI). 8-bromoadenosine 3',5'-cyclic monophosphorothioate, Sp-isomer and acetoxymethyl ester (Sp-8-Br-cAMPS-AM, 10 mM in DMSO) was from BIOLOG LSI (Bremen, DE).

Animals

Male Sprague Dawley rats (200-225 g, aged 8-10 weeks) were obtained from Harlan (Rossdorf, DE). Conditional $Na_v1.7$ knockout mice were generated by crossing floxed (SCN9A) $Na_v1.7$ mice with Advillin-Cre mice (10, 32) and global Nav1.8 knockout mice were used (25). Female and male mice were aged between 6–20 weeks. Mice and rats were kept on a 12-h light/dark cycle and provided with food and water *ad libitum*. All animal experiments were performed in accordance with the German animal welfare law and approved by the Landesamt für Natur, Umwelt und Verbraucherschutz Nordrhein-Westfalen or approved by the United Kingdom Home Office according to guidelines set by personal

and project licenses, as well as guidelines of the Committee for Research and Ethical Issues of IASP. Animals were sacrificed between 9-12 a.m. by CO_2 intoxication. Dorsal root ganglion from rats (L1-L6) or mice (lumbar and thoracic) were removed within 30 min per animal.

Dorsal root ganglion neuron cultures

Dorsal root ganglion were de-sheathed, pooled, and incubated in Neurobasal A/B27 medium (Invitrogen, Carlsbad, CA) containing collagenase P (Roche, Penzberg, DE) (0.2 U/ml, 1 h, 37 C, 5% CO_2). The dorsal root ganglion were dissociated by trituration with fire-polished Pasteur pipettes. Axon stumps and disrupted cells were removed by bovine serum albumin (BSA) gradient centrifugation (15% BSA, 120 *g*, 8 min). Viable cells were resuspended in Neurobasal A/B27 medium, plated in poly-L-ornithine (0.1 mg/ml)/laminin (5 µg/ml)-precoated 96-well imaging plates (Greiner, Kremsmünster, AU) and incubated overnight (37 °C, 5% CO_2). Neuron density was 1500 neurons/cm^2.

Stimulation of dorsal root ganglion neurons

Dorsal root ganglion neurons were stimulated 24 hours after isolation in 96-well imaging plates. Compounds were dissolved in 12.5 µl PBS, pH 7.4, in 96-well V-bottom plates, mixed with 50 µl medium from the culture wells, and added back to the same wells. Stimulations were performed with automated 8 channel pipettes (Eppendorf, Hamburg, DE) at low dispense speed on heated blocks, stimulated cells were placed back in the incubator. The cells were fixed for 10 minutes at room temperature (RT) by adding 100 µl 8% paraformaldehyde resulting in a final concentration of 4%.

Immunofluorescence staining

Fixed cells were treated with goat serum blocking solution (2% goat serum, 1% BSA, 0.1% Triton X-100, 0.05% Tween 20, 1h, RT) and incubated with respective primary antibodies diluted in 1% BSA in PBS, pH7.4, at 4 °C overnight. After three washes with PBS (30 min, RT), cells were incubated with secondary Alexa dye-coupled antibodies (1:1000, 1h, RT). After three final washes (30 min, RT), wells of 96-well plates were filled with PBS, sealed, and stored at 4 °C until scanning.

Quantitative microscopy

Stained dorsal root ganglion cultures in 96-well plates were scanned using a Cellomics ArrayScan XTI with an LED light source. Images of 1024 x 1024 pixels were acquired with a 10x objective and analyzed using the Cellomics software package. Briefly, images of UCHL1 staining were background corrected (low pass filtration), converted to binary image masks (fixed threshold), segmented (geometric method), and neurons were identified by the object selection parameters size: 80-7500 μm^2; circularity (perimeter^2 / 4π area): 1-3; length-to-width ratio: 1-2; average intensity: 800-12000,;and total intensity: 2×10^5-5×10^7. These image masks were then overlaid on images obtained at other fluorescence wavelengths to quantify signal intensities. To calculate spill-over between fluorescence channels, three respective controls were prepared for each triple staining: (i) UCHL1 alone, (ii) UCHL1 + antibody 1, and (iii) UCHL1 + antibody 2. Raw fluorescence data of the

controls were used to calculate the slope of best fit straight lines by linear regression, which was then used to compensate spill-over as described previously (45). Compensated data were scaled to a mean value of 1 (or 1000) for the unstimulated cells to adjust for variability between experimental days. One and two-dimensional probability density plots were generated using R packages (46). Gating of subpopulations was performed by setting thresholds at local minima of probability density plots. The mean number of analyzed neurons was 31,288 ± 3231 (L1-L6 only) per rat and 30965 ± 1438 per mouse (lumbar and thoracic dorsal root ganglion).

Electrophysiology

All electrophysiological recordings were performed using an AxoPatch 200B amplifier and a Digidata 1440A digitiser (Axon Instruments), controlled by Clampex software (version 10, Molecular Devices). Filamented borosilicate microelectrodes (GC150TF-7.5, Harvard Apparatus) were coated with beeswax and fire polished using a microforge (Narishige) to give resistances of 2-3 MΩ. For voltage-clamp experiments, the following solutions were used. Extracellular solution (values are in mM): 70 NaCl, 70 Choline.Cl, 3 KCl, 1 $MgCl_2$, 1 $CaCl_2$, 20 tetraethylammonium (TEA).Cl, 0.1 $CdCl_2$, 0.3 tetrodotoxin (TTX), 10 HEPES, 10 glucose, pH 7.3 with NaOH. Intracellular solution (values are in mM): 140 CsF, 1 EGTA, 10 NaCl, 10 HEPES, pH 7.3 with CsOH. Unless otherwise stated standard whole-cell currents were acquired at 25 kHz and filtered at 10 kHz (low-pass Bessel filter). After achieving whole-cell configuration the cell was left for five minutes to dialyze the intracellular solution. A holding potential of -100 mV was applied and series resistance was compensated by ≥ 70%. All currents were leak subtracted using a p/4 protocol. To record TTXr sodium currents, a depolarizing voltage-pulse protocol was applied to cell; the cell was held at -100 mV and then stepped to -15 mV for 50 ms before returning back to -100 mV. This step was applied every 5 seconds for the duration of the experiment. The cells were continuously perfused using a gravity-fed perfusion system. All electrophysiological data were extracted using Clampfit (version 10, Molecular Devices) and analyzed using GraphPad Prism software (version 6, GraphPad Software).

Statistical Analysis

Statistical analyses were performed with Students t-tests, one-, or two-way ANOVA with respective post hoc tests as indicated in the figure legends. $P < 0.05$ was considered statistically significant. Dose-response curves from HCS microscopy were generated using non-linear regression curve-fitting (three parameter, standard Hill slope) with Prism (GraphPad, La Jolla, CA). The parameters of the model (top, bottom, or pEC_{50}/pIC_{50} values) were compared using the extra-sum-of-squares F test. High content screening kinetic experiments were analyzed with R (46) using ordinary two-way ANOVA. Bonferroni's post hoc analysis was applied to determine *P* values of selected pairs defined in a contrast matrix using the R library multcomp. Error bars represent the standard error of the mean (SEM) of 3-5 independent replicate experiments using cells of different animals.

Supplementary Material

Refer to Web version on PubMed Central for supplementary material.

Acknowledgments

We thank M. Siobal, J. Klimek, and H. Hammerich for excellent technical support.

Funding: J.I., L.K., and T.H. were supported by grants from the Federal Ministry of Education and Research, Germany [NoPain (FKZ0316177A)]. K.M. was supported by the Evangelisches Studienwerk Villigst and the graduate program in Pharmacology and Experimental Therapeutics at the University of Cologne, which was financially and scientifically supported by Bayer. J.S., E.E., V.P., X.S., and J.N.W. were supported by the Wellcome Trust and Arthritis Research, UK.

References

1. Gaskin DJ, Richard P. The economic costs of pain in the United States. J Pain. 2012; 13:715. [PubMed: 22607834]
2. Turk DC, Wilson HD, Cahana A. Treatment of chronic non-cancer pain. Lancet. 2011; 377:2226. [PubMed: 21704872]
3. McNicol ED, Midbari A, Eisenberg E. Opioids for neuropathic pain. The Cochrane database of systematic reviews. 2013; 8doi: 10.1002/14651858.CD006146.pub2
4. Chaparro LE, Furlan AD, Deshpande A, Mailis-Gagnon A, Atlas S, Turk DC. Opioids compared to placebo or other treatments for chronic low-back pain. Cochrane Database Syst Rev. 2013; 8
5. Reinecke H, Weber C, Lange K, Simon M, Stein C, Sorgatz H. Analgesic efficacy of opioids in chronic pain: recent meta-analyses. Br J Pharmacol. 2015; 172:324. [PubMed: 24640991]
6. Woodcock J. A difficult balance--pain management, drug safety, and the FDA. The New England journal of medicine. 2009; 361:2105. [PubMed: 19940297]
7. Manchikanti L, Helm S 2nd, Fellows B, Janata JW, Pampati V, Grider JS, Boswell MV. Opioid epidemic in the United States. Pain Physician. 2012; 15:ES9–ES38. [PubMed: 22786464]
8. Williams JT, Ingram SL, Henderson G, Chavkin C, von Zastrow M, Schulz S, Koch T, Evans CJ, Christie MJ. Regulation of mu-opioid receptors: desensitization, phosphorylation, internalization, and tolerance. Pharmacol Rev. 2013; 65:223. [PubMed: 23321159]
9. Cox JJ, Reimann F, Nicholas AK, Thornton G, Roberts E, Springell K, Karbani G, Jafri H, Mannan J, Raashid Y, Al-Gazali L, et al. An SCN9A channelopathy causes congenital inability to experience pain. Nature. 2006; 444:894. [PubMed: 17167479]
10. Minett MS, Nassar MA, Clark AK, Passmore G, Dickenson AH, Wang F, Malcangio M, Wood JN. Distinct Nav1.7-dependent pain sensations require different sets of sensory and sympathetic neurons. Nat Commun. 2012; 3:791. [PubMed: 22531176]
11. Gingras J, Smith S, Matson DJ, Johnson D, Nye K, Couture L, Feric E, Yin R, Moyer BD, Peterson ML, Rottman JB, et al. Global Nav1.7 knockout mice recapitulate the phenotype of human congenital indifference to pain. PLoS One. 2014; 9:e105895. [PubMed: 25188265]
12. Waxman SG, Zamponi GW. Regulating excitability of peripheral afferents: emerging ion channel targets. Nat Neurosci. 2014; 17:153. [PubMed: 24473263]
13. Emery EC, Luiz AP, Wood JN. Na1.7 and other voltage-gated sodium channels as drug targets for pain relief. Expert Opin Ther Targets. 2016; 20:975–983. [PubMed: 26941184]
14. Schmalhofer WA, Calhoun J, Burrows R, Bailey T, Kohler MG, Weinglass AB, Kaczorowski GJ, Garcia ML, Koltzenburg M, Priest BT. ProTx-II, a selective inhibitor of NaV1.7 sodium channels, blocks action potential propagation in nociceptors. Molecular pharmacology. 2008; 74:1476. [PubMed: 18728100]
15. Minett MS, Pereira V, Sikandar S, Matsuyama A, Lolignier S, Kanellopoulos AH, Mancini F, Iannetti GD, Bogdanov YD, Santana-Varela S, Millet Q, et al. Endogenous opioids contribute to insensitivity to pain in humans and mice lacking sodium channel Nav1.7. Nat Commun. 2015; 6:8967. [PubMed: 26634308]
16. Dumuis A, Bouhelal R, Sebben M, Cory R, Bockaert J. A nonclassical 5-hydroxytryptamine receptor positively coupled with adenylate cyclase in the central nervous system. Mol Pharmacol. 1988; 34:880–887. [PubMed: 2849052]

17. Cardenas LM, Cardenas CG, Scroggs RS. 5HT increases excitability of nociceptor-like rat dorsal root ganglion neurons via cAMP-coupled TTX-resistant Na(+) channels. J Neurophysiol. 2001; 86:241. [PubMed: 11431505]
18. Borsodi, A; Caló, G; Chavkin, C; Christie, MJ; Civelli, O; Cox, BM; Devi, LA; Evans, C; Henderson, G; Höllt, V; Kieffer, B; , et al. Opioid receptors: μ receptor. IUPHAR/BPS Guide to PHARMACOLOGY. 2016. www.guidetopharmacology.org/GRAC/ObjectDisplayForward?objectId=319
19. Isensee J, Diskar M, Waldherr S, Buschow R, Hasenauer J, Prinz A, Allgower F, Herberg FW, Hucho T. Pain modulators regulate the dynamics of PKA-RII phosphorylation in subgroups of sensory neurons. J Cell Sci. 2014; 127:216. [PubMed: 24190886]
20. Akopian AN, Souslova V, England S, Okuse K, Ogata N, Ure J, Smith A, Kerr BJ, McMahon SB, Boyce S, Hill R, et al. The tetrodotoxin-resistant sodium channel SNS has a specialized function in pain pathways. Nat Neurosci. 1999; 2:541. [PubMed: 10448219]
21. Alexander SPH, Benson HE, Faccenda E, Pawson AJ, Sharman JL, Spedding M, Peters JA, Harmar AJ, Collaborators C. The Concise Guide to PHARMACOLOGY 2013/14: G protein-coupled receptors. Br J Pharmacol. 2013; 170:1459. [PubMed: 24517644]
22. Cardenas CG, Del Mar LP, Cooper BY, Scroggs RS. 5HT4 receptors couple positively to tetrodotoxin-insensitive sodium channels in a subpopulation of capsaicin-sensitive rat sensory neurons. J Neurosci. 1997; 17:7181. [PubMed: 9295364]
23. Zhang P, Knape MJ, Ahuja LG, Keshwani MM, King CC, Sastri M, Herberg FW, Taylor SS. Single Turnover Autophosphorylation Cycle of the PKA RIIbeta Holoenzyme. PLoS biology. 2015; 13:e1002192. [PubMed: 26158466]
24. Isensee J, Wenzel C, Buschow R, Weissmann R, Kuss AW, Hucho T. Subgroup-Elimination Transcriptomics Identifies Signaling Proteins that Define Subclasses of TRPV1-Positive Neurons and a Novel Paracrine Circuit. PLoS One. 2014; 9:e115731. [PubMed: 25551770]
25. Flynn DL, Zabrowski DL, Becker DP, Nosal R, Villamil CI, Gullikson GW, Moummi C, Yang DC. SC-53116: the first selective agonist at the newly identified serotonin 5-HT4 receptor subtype. Journal of medicinal chemistry. 1992; 35:1486. [PubMed: 1573641]
26. Torres GE, Holt IL, Andrade R. Antagonists of 5-HT4 receptor-mediated responses in adult hippocampal neurons. J Pharmacol Exp Ther. 1994; 271:255. [PubMed: 7965722]
27. Usoskin D, Furlan A, Islam S, Abdo H, Lonnerberg P, Lou D, Hjerling-Leffler J, Haeggstrom J, Kharchenko O, Kharchenko PV, Linnarsson S, et al. Unbiased classification of sensory neuron types by large-scale single-cell RNA sequencing. Nat Neurosci. 2015; 18:145. [PubMed: 25420068]
28. Sharma SK, Klee WA, Nirenberg M. Dual regulation of adenylate cyclase accounts for narcotic dependence and tolerance. Proc Natl Acad Sci U S A. 1975; 72:3092. [PubMed: 1059094]
29. Johnston CA, Beazely MA, Vancura AF, Wang JK, Watts VJ. Heterologous sensitization of adenylate cyclase is protein kinase A-dependent in Cath.a differentiated (CAD)-D2L cells. J Neurochem. 2002; 82:1087. [PubMed: 12358756]
30. Cahill CM, Walwyn W, Taylor AM, Pradhan AA, Evans CJ. Allostatic Mechanisms of Opioid Tolerance Beyond Desensitization and Downregulation. Trends in pharmacological sciences. 2016; 37:963. [PubMed: 27670390]
31. Stefan E, Malleshaiah MK, Breton B, Ear PH, Bachmann V, Beyermann M, Bouvier M, Michnick SW. PKA regulatory subunits mediate synergy among conserved G-protein-coupled receptor cascades. Nat Commun. 2011; 2:598. [PubMed: 22186894]
32. England S, Bevan S, Docherty RJ. PGE2 modulates the tetrodotoxin-resistant sodium current in neonatal rat dorsal root ganglion neurones via the cyclic AMP-protein kinase A cascade. J Physiol. 1996; 495(Pt 2):429. [PubMed: 8887754]
33. Fitzgerald EM, Okuse K, Wood JN, Dolphin AC, Moss SJ. cAMP-dependent phosphorylation of the tetrodotoxin-resistant voltage-dependent sodium channel SNS. J Physiol. 1999; 516:433. [PubMed: 10087343]
34. Nassar MA, Stirling LC, Forlani G, Baker MD, Matthews EA, Dickenson AH, Wood JN. Nociceptor-specific gene deletion reveals a major role for Nav1.7 (PN1) in acute and inflammatory pain. Proc Natl Acad Sci U S A. 2004; 101:12706. [PubMed: 15314237]

35. Bouras EP, Camilleri M, Burton DD, McKinzie S. Selective stimulation of colonic transit by the benzofuran 5HT4 agonist, prucalopride, in healthy humans. Gut. 1999; 44:682. [PubMed: 10205205]
36. Sakurai-Yamashita Y, Yamashita K, Kanematsu T, Taniyama K. Localization of the 5-HT(4) receptor in the human and the guinea pig colon. Eur J Pharmacol. 1999; 383:281. [PubMed: 10594320]
37. Manzke T, Guenther U, Ponimaskin EG, Haller M, Dutschmann M, Schwarzacher S, Richter DW. 5-HT4(a) receptors avert opioid-induced breathing depression without loss of analgesia. Science. 2003; 301:226. [PubMed: 12855812]
38. Millan MJ. Descending control of pain. Progress in neurobiology. 2002; 66:355. [PubMed: 12034378]
39. Driessen B, Reimann W. Interaction of the central analgesic, tramadol, with the uptake and release of 5-hydroxytryptamine in the rat brain in vitro. Br J Pharmacol. 1992; 105:147. [PubMed: 1596676]
40. Kolesnikov YA, Chereshnev I, Pasternak GW. Analgesic synergy between topical lidocaine and topical opioids. J Pharmacol Exp Ther. 2000; 295:546. [PubMed: 11046087]
41. Pert CB, Pasternak G, Snyder SH. Opiate agonists and antagonists discriminated by receptor binding in brain. Science. 1973; 182:1359. [PubMed: 4128222]
42. Katritch V, Fenalti G, Abola EE, Roth BL, Cherezov V, Stevens RC. Allosteric sodium in class A GPCR signaling. Trends Biochem Sci. 2014; 39:233. [PubMed: 24767681]
43. Fenalti G, Giguere PM, Katritch V, Huang XP, Thompson AA, Cherezov V, Roth BL, Stevens RC. Molecular control of delta-opioid receptor signalling. Nature. 2014; 506:191. [PubMed: 24413399]
44. Livingston KE, Traynor JR. Disruption of the Na+ ion binding site as a mechanism for positive allosteric modulation of the mu-opioid receptor. Proc Natl Acad Sci U S A. 2014; 111:18369. [PubMed: 25489080]
45. Chattopadhyay M, Mata M, Fink DJ. Continuous delta-opioid receptor activation reduces neuronal voltage-gated sodium channel (NaV1.7) levels through activation of protein kinase C in painful diabetic neuropathy. J Neurosci. 2008; 28:6652. [PubMed: 18579738]
46. Chattopadhyay M, Zhou Z, Hao S, Mata M, Fink DJ. Reduction of voltage gated sodium channel protein in DRG by vector mediated miRNA reduces pain in rats with painful diabetic neuropathy. Mol Pain. 2012; 8:17. [PubMed: 22439790]
47. Roederer M. Compensation in flow cytometry. Curr Protoc Cytom. 2002; Chapter 1:Unit 1.14.
48. R. D. C. Team. R: A Language and Environment for Statistical Computing. R. F. f. S. Computing; Vienna: 2011.

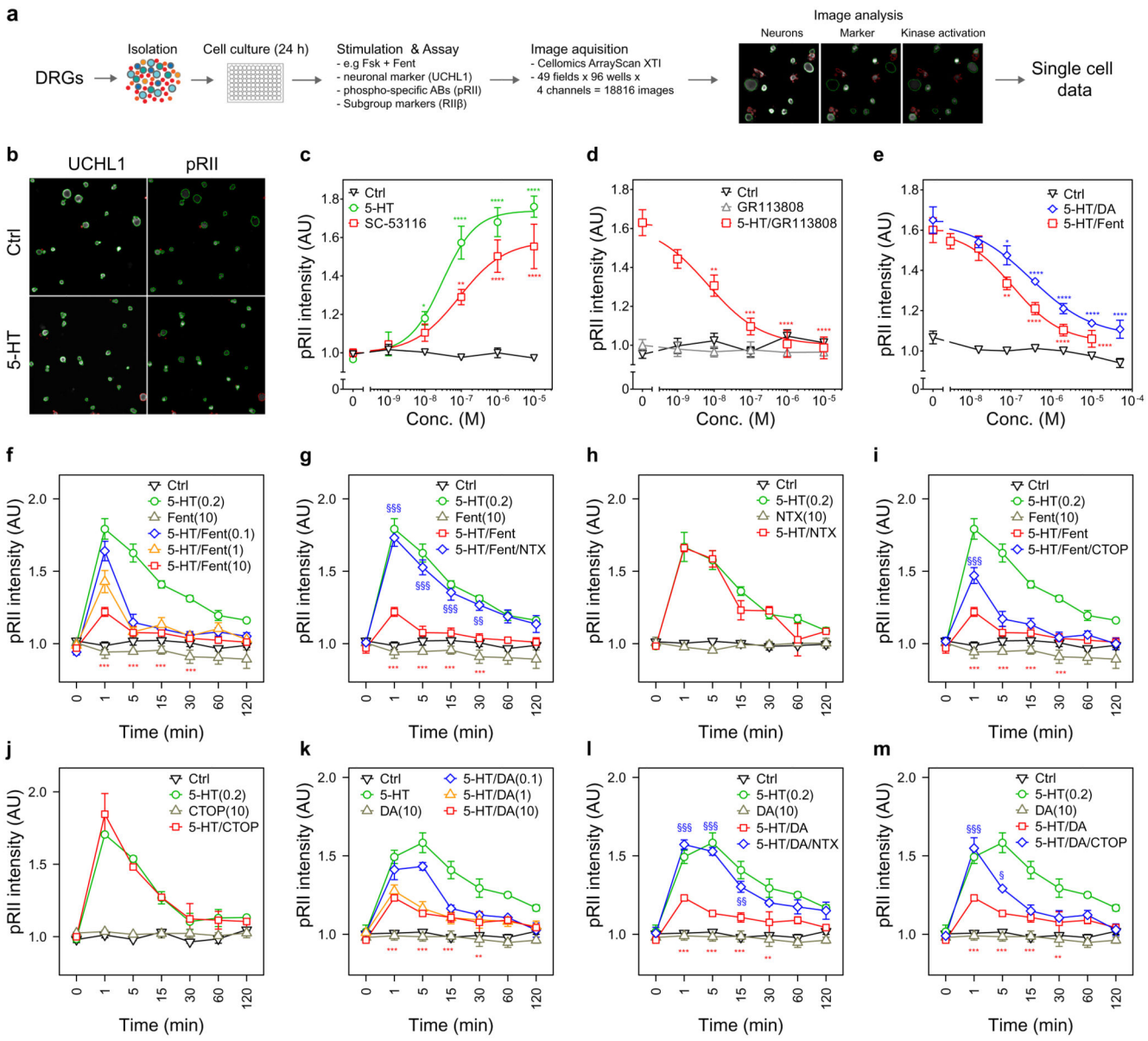

Fig. 1. 5-HT-induced increase of pRII is mediated by 5-HT$_4$ receptors and inhibited by opioids in rat sensory neurons.

(A) Representative images of rat sensory neurons from dorsal root ganglion that were stimulated with solvent (control, Ctrl) or 5-HT (0.2 μM) for 3 min. Cultures were stained with UCHL1 to identify the neurons and pRII to quantify PKA-II signaling activity. Green or red encircled neurons indicate automatically selected or rejected objects, respectively. Scale bar, 100 μm. **(B)** Dose response curve showing the pRII intensities in selected neurons exposed to 5-HT (0-10 μM, EC_{50} = 30 nM) or the 5-HT$_4$-specific agonist SC-53116 (0-10 μM, EC_{50} = 89 nM) for 3 min. **(C)** Dose response curve showing the effect of the 5-HT$_4$-specific antagonist GR113808 (0-10 μM, IC_{50} = 8.6 nM) on pRII signals induced by 5-HT (0.2 μM). 5-HT and GR113808 were applied simultaneously. **(D)** Dose response curve showing the effect of fentanyl (Fent, 0-10 μM, IC_{50} = 97 nM) or the MOR-specific agonist

DAMGO (DA, 0-50 μM, IC_{50} = 321 nM) on pRII signals induced by 5-HT (0.2 μM) (Difference of pIC_{50}: $F_{1,47}$ = 4.2, n = 4, P < 0.05, extra-sum-of-squares F test). **(E)** Time-course experiment showing the dose-dependent effect of fentanyl on pRII signals induced by 5-HT (Dose effect: $F_{3,84}$ = 77.2, n = 4, P < 2e-16). **(F)** Time-course experiment showing the effect of the opioid receptor antagonist naltrexone (NTX, 10 μM) on the inhibition of the 5-HT-induced pRII signal by fentanyl ($F_{1,42}$ = 136, n = 4, P < 9.5e-15). **(G)** The effect of naltrexone on the baseline or 5-HT-induced pRII signal. **(H)** The effect of the MOR antagonist CTOP (10 μM) on the inhibition of the 5-HT-induced pRII signal by fentanyl ($F_{1,42}$ = 12, n = 4, P < 0.01). **(I)** The effect of CTOP on the baseline or 5-HT-induced pRII signal. **(J)** The effect of DAMGO on the 5-HT-induced pRII signal (Dose effect: $F_{3,56}$ = 51, n = 3, P < 5e-16). **(K** and **L)** Effect of naltrexone and CTOP on the inhibition of the 5-HT-induced pRII signal by DAMGO. In (B) to (L), concentrations are indicated in micromolar; control conditions were treated with solvent; data are presented as means ± SEM; n = 3 to 4 independent experiments; >2000 neurons/condition; two-way ANOVA with Bonferroni's test; *P<0.05; **P<0.01; ***P<0.001 indicate significance levels between baseline and stimulated conditions; $^{§}P$<0.05; $^{§§}P$<0.01; $^{§§§}P$<0.001 indicate significance levels between stimulated and inhibited conditions.

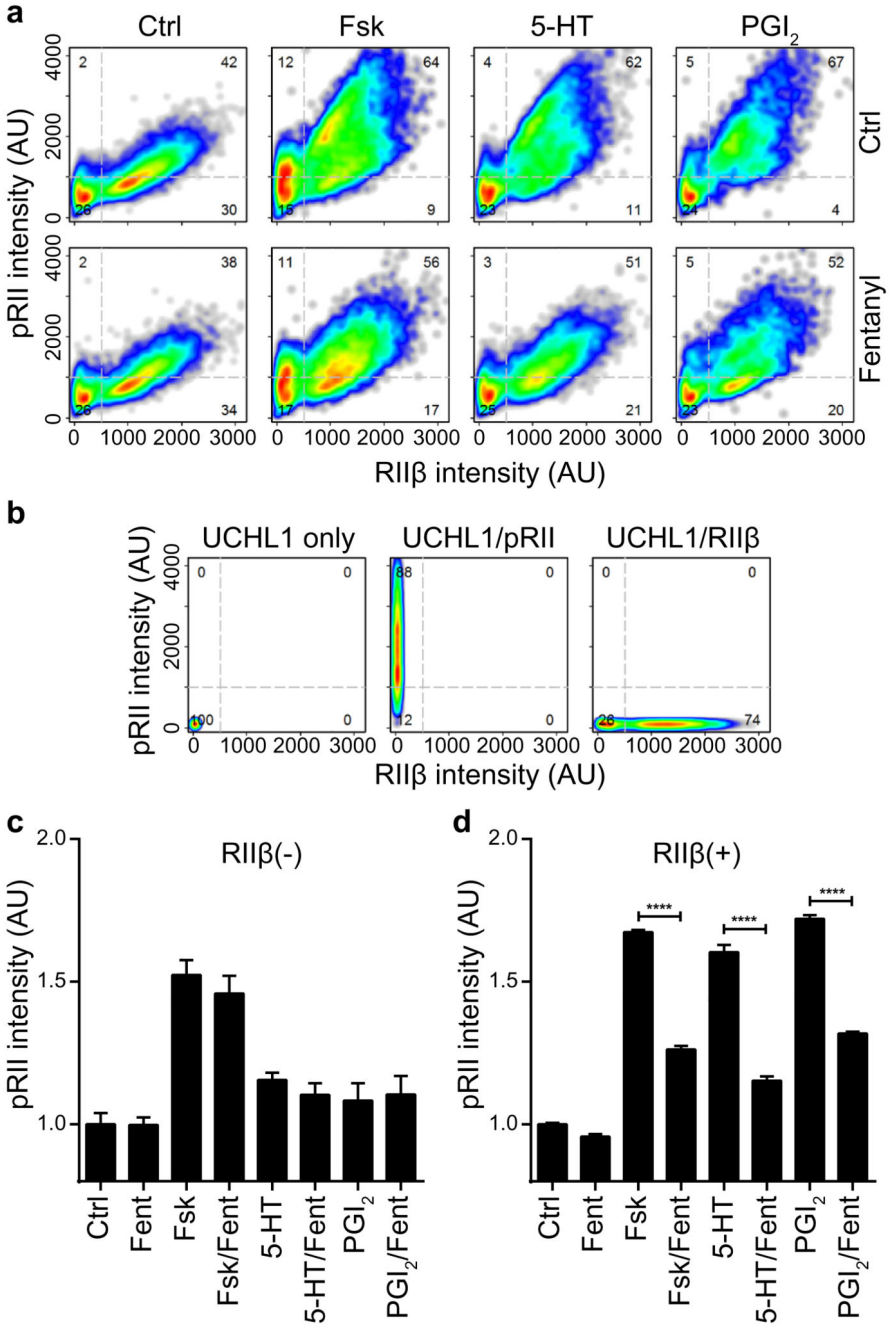

Fig. 2. Opioids inhibit pRII-increases selectively in RIIβ(+) sensory neurons of rats.

(A) Cell density plots showing single cell data of pRII/RIIβ-labeled rat sensory neurons stimulated with Fsk (2 μM), 5-HT (0.2 μM), or PGI_2 (1 μM) in the absence (top) or presence (bottom) of fentanyl (2 μM). Dashed lines indicate gating thresholds to discriminate between RIIβ(-) and RIIβ(+) neurons with the numbers indicating the relative percentage of cells in the respective quadrant. Combined data of $n = 4$ experiments with a total of >8000 neurons/condition. **(B)** Compensation controls showing removal of spill-over between fluorescence channels. The graphs show the pRII versus the RIIβ intensity in control samples stained with

UCHL1 alone (left), UCHL1 and pRII (middle), or UCHL1 and RIIβ (right) after compensation has been applied. **(C)** Normalized mean pRII intensities in RIIβ(-) (left) and RIIβ(+) (right) neurons. Values are means ± SEM; $n = 4$ independent experiments; >8000 neurons/condition; two-way ANOVA with Bonferroni's test; *$P<0.05$; **$P<0.01$; ***$P<0.001$; ****$P<0.0001$.

Europe PMC Funders Author Manuscripts

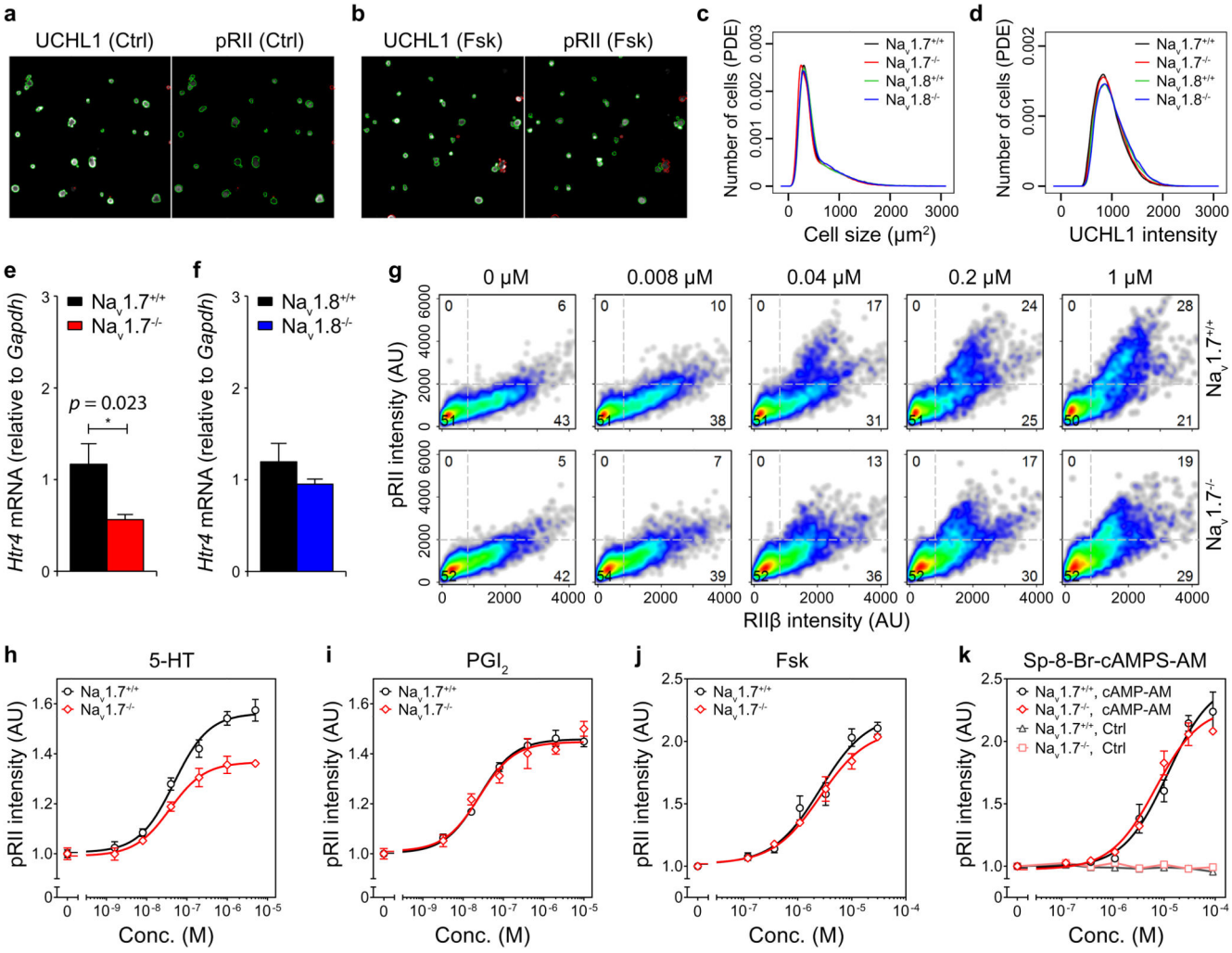

Fig. 3. Loss of $Na_V1.7$ results in a decrease in 5-HT_4 receptor abundance and reduced 5-HT-induced increase in pRII.

(A) Representative images of solvent (Ctrl, left) and forskolin (Fsk, right) stimulated sensory neurons from adult wild-type (WT) mice. Green or red encircled neurons indicate inclusion or rejection of objects, respectively, for quantification. Scale bar, 100 µm. **(B)** Size and UCHL1 intensity distributions of sensory neurons from $Na_V1.7^{-/-}$ and $Na_V1.8^{-/-}$ mice. Probability density estimates (PDE) are from $>10^5$ neurons analyzed in $n = 4$ independent experiments (2 males and 2 females per genotype). **(C)** Real-time PCR quantification of *Htr4* mRNA encoding 5-HT_4 receptors in $Na_V1.7^{-/-}$ and $Na_V1.8^{-/-}$ mice versus WT controls. Data are means ± SEM; $n = 6$ (three males and three females per genotype), Student's unpaired t-test. **(D)** Single cell data of pRII/RIIβ-labeled sensory neurons after 3 min stimulation with increasing doses of 5-HT. Combined data of >3000 neurons/condition from $n = 5$ females per genotype. Numbers of RIIβ(+) neurons responsive to 5-HT (1 µM, upper right quadrant) were 27.8 ± 1.3% in $Na_V1.7^{+/+}$ versus 19.1 ± 1.2% in $Na_V1.7^{-/-}$ mice (n = 5, $P < 0.001$, Student's t-test). **(E)** Dose-response curves showing the effect of GPCR agonists 5-HT (0-5 µM) and PGI_2 (0-10 µM), stimulator of adenylyl cyclase Fsk (0-30 µM), or cAMP analog Sp-8-Br-cAMPS-AM (0-30 µM) on pRII signals in sensory neurons from each

genotype. Data are means ± SEM; $n = 5$ females per genotype; genotype effect for 5-HT: $F_{1,64} = 53.6$, n = 5, $P < 0.0001$ at 1-5 μM; extra-sum-of-squares F test.

Europe PMC Funders Author Manuscripts

Europe PMC Funders Author Manuscripts

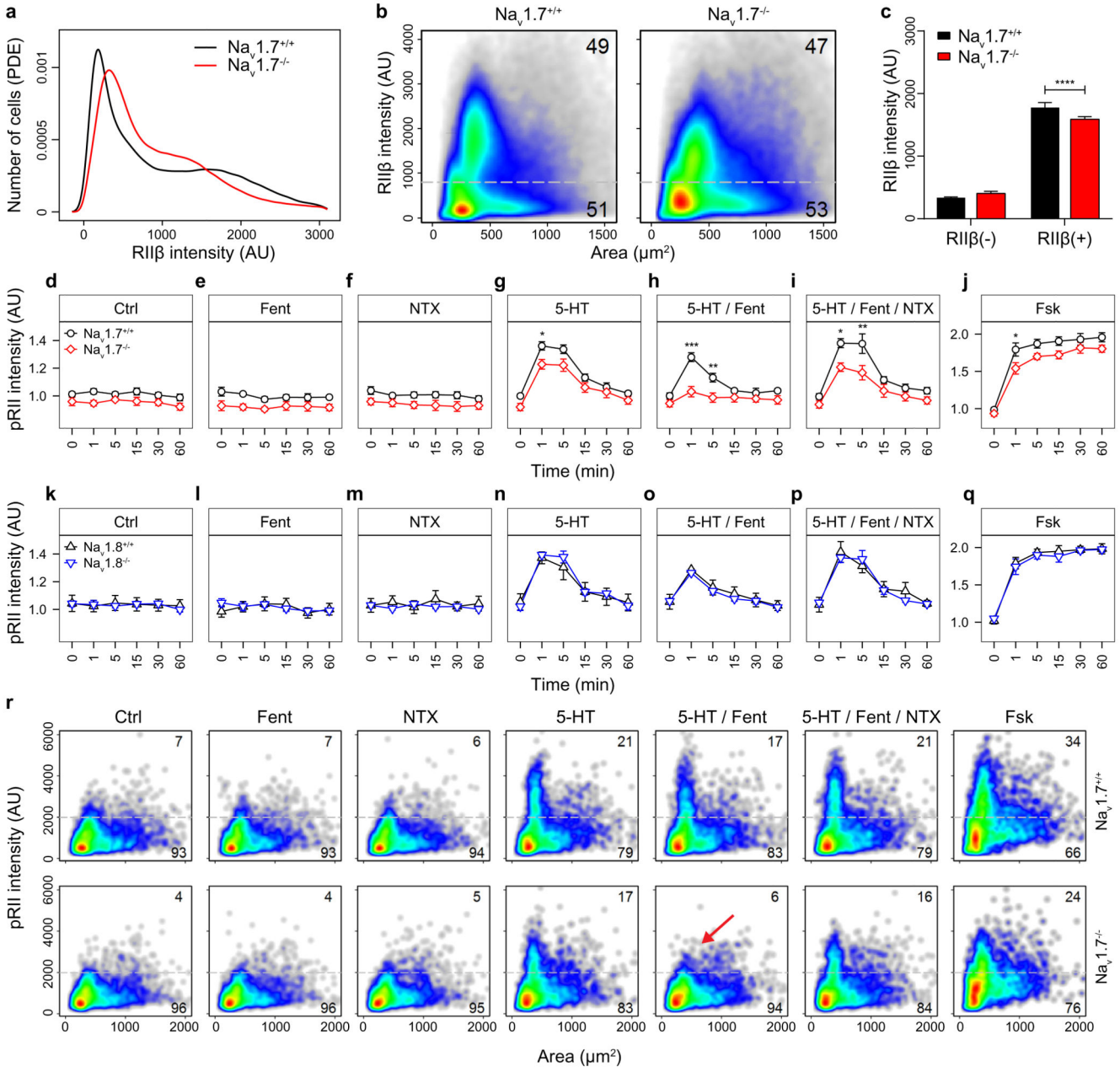

Fig. 4. Sensory neurons of $Na_V1.7^{-/-}$ but not $Na_V1.8^{-/-}$ mice have a lower basal pRII and exhibit a stronger response to the opioid receptor agonist fentanyl.

(A) Time-course of pRII intensity after stimulation of sensory neurons from Nav1.7$^{-/-}$ mice and WT controls (Nav1.7$^{+/+}$) with fentanyl (Fen, 2 µM), naltrexone (NTX, 10 µM), serotonin (5-HT, 0.2 µM), combinations thereof, or forskolin (Fsk, 10 µM). Basal pRII intensity was 8% lower in sensory neurons from Nav1.7$^{-/-}$ mice (Genotype effect in Ctrl: $F_{1,36}$ = 22.9, n = 4, P < 3e-05). The inhibitory effect of fentanyl was greater in sensory neurons of Nav1.7$^{-/-}$ mice ($F_{1,35}$ = 37, n = 4, P < 6e-07). **(B)** Time-course of pRII intensity after stimulation of sensory neurons from Nav1.8$^{-/-}$ mice and WT controls (Nav1.8$^{+/+}$) with the same compounds as in A. **(C)** Cell density plots showing single cell data of RIIβ-labeled

sensory neurons from Nav1.7$^{-/-}$ mice and WT controls. The threshold (grey dashed line) discriminates between RIIβ(-) and RIIβ(+) neurons. Data represent >10^5 neurons/plot; n = 5 females per genotype. **(D)** Distribution of RIIβ expression in sensory neurons of $Na_v1.7$-deficient mice (red line) and WT littermates (black line). **(E)** Mean RIIβ intensities were 11% lower in RIIβ(+) neurons of $Na_v1.7^{-/-}$ mice compared to WT littermates (1589 ± 19 vs. 1779 ± 34, n = 5, P < 0.0001, two-way ANOVA with Bonferroni's test). **(F)** Density plots of pRII intensity vs. cell size showing single cell data of all neurons shown in A after 1 min stimulation. Threshold (grey dashed lines) were used to estimate the number of responsive cells. Data in A and B are means ± SEM; n = 4 (2 males and 2 females per genotype); >3000 neurons/condition; two-way ANOVA with Bonferroni's test; *P<0.05; **P<0.01; ***P<0.001, ****p<0.0001.

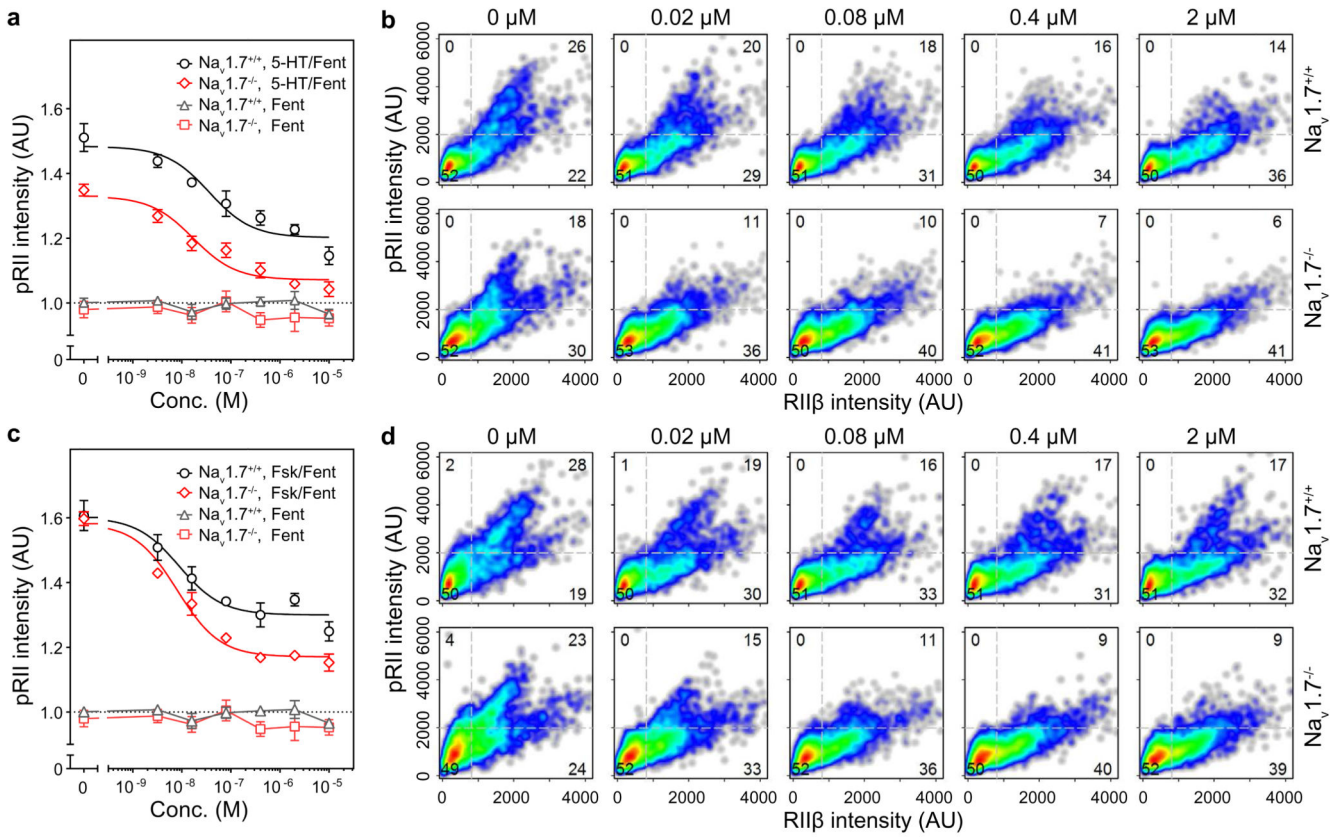

Fig. 5. The ability of opioids to inhibit 5-HT- or Fsk-induced increase in pRII is enhanced in $Na_v1.7^{-/-}$ mice.

(A) Dose-response relationship of pRII intensities showing the effect of fentanyl (0-10 μM) on the 5-HT response (0.2 μM) after 3 min stimulation of dorsal root ganglion neurons from $Na_v1.7$-deficient mice and WT litters ($Na_v1.7^{+/+}$). Data are means ± SEM; genotype effect: $F_{2,56} = 13.6$, $n = 4$ females per genotype; $P < 0.0001$ for whole curve; extra-sum-of-squares F test. **(B)** Combined single cell data of pRII/RIIβ-labeled sensory neurons shown in (A) representing >2500 neurons/condition. **(C)** Dose-response relationship of pRII intensities in sensory neurons of $Na_v1.7^{-/-}$ and $Na_v1.7^{+/+}$ mice stimulated for 3 min with increasing doses of fentanyl (0-10 μM) in the presence of Fsk (2 μM). Data are means ± SEM; genotype effect: $F_{1,50} = 32$; $n = 4$ females per genotype; $P<0.0001$ for bottom values (0.4-10 μM); extra-sum-of-squares F test. **(D)** Combined single cell data of pRII/RIIβ-labeled sensory neurons shown in (C) representing >2500 neurons per condition.

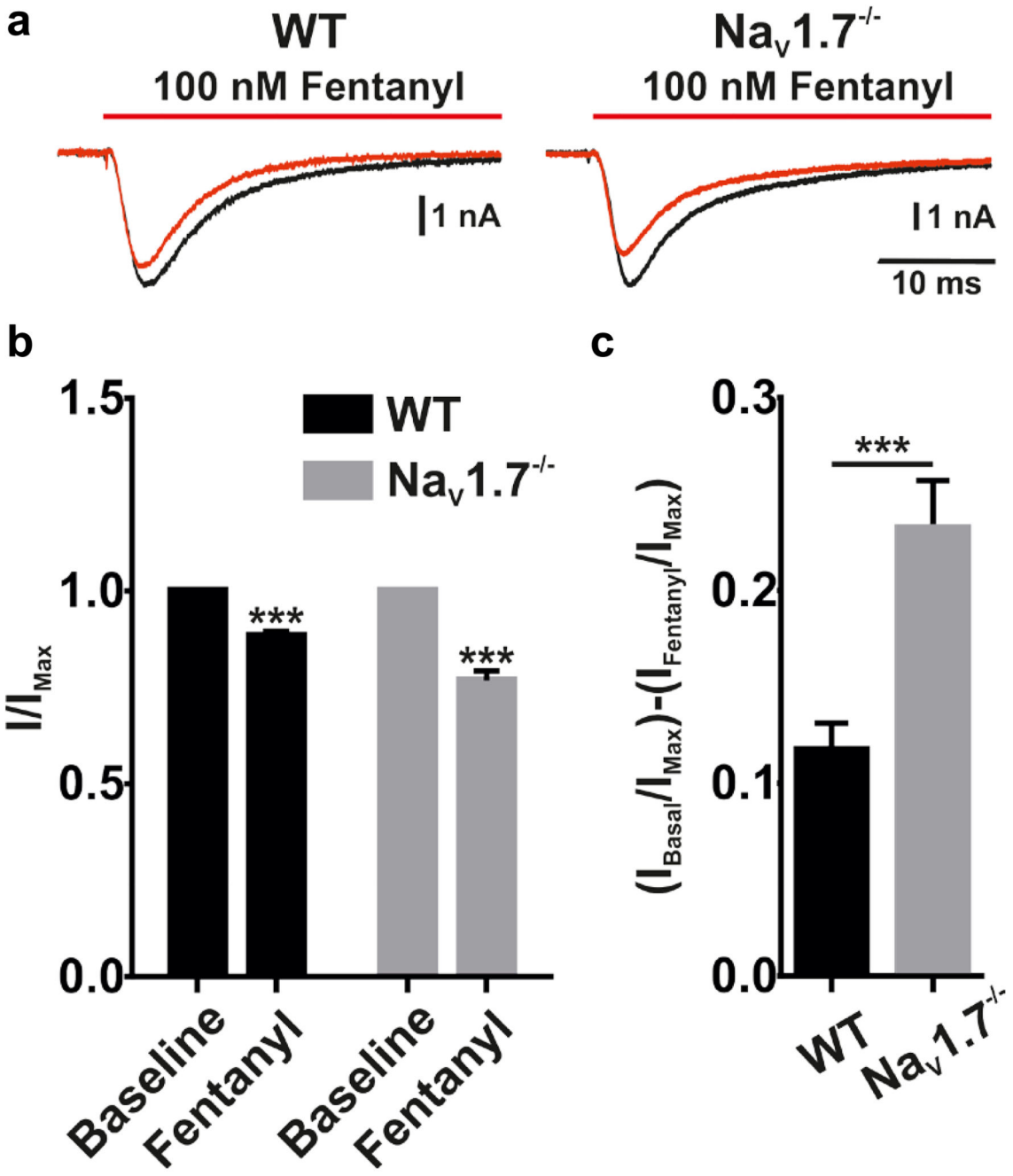

Fig. 6. Effect of fentanyl on TTXr Na^+ currents from $Na_v1.7^{+/+}$ and $Na_v1.7^{-/-}$ sensory neurons.

(A) Electrophysiological current recording showing TTXr Na+ current before (black) and after (red) the application of fentanyl (100 nM) in $Na_v1.7^{+/+}$ and $Na_v1.7^{-/-}$ dorsal root ganglion neurons. **(B)** Change in peak current (%) of TTXr Na^+ current after the application of fentanyl in $Na_v1.7^{+/+}$ and $Na_v1.7^{-/-}$ dorsal root ganglion neurons. **(C)** Average change in TTXr Na+ peak current (%) in $Na_v1.7^{+/+}$ and $Na_v1.7^{-/-}$ dorsal root ganglion neurons after addition of 100 nM fentanyl. Data in (B) and (C) represent mean ± SEM; $n = 9$ neurons per genotype; Student's unpaired t-test; ***$P<0.001$.

Europe PMC Funders Author Manuscripts

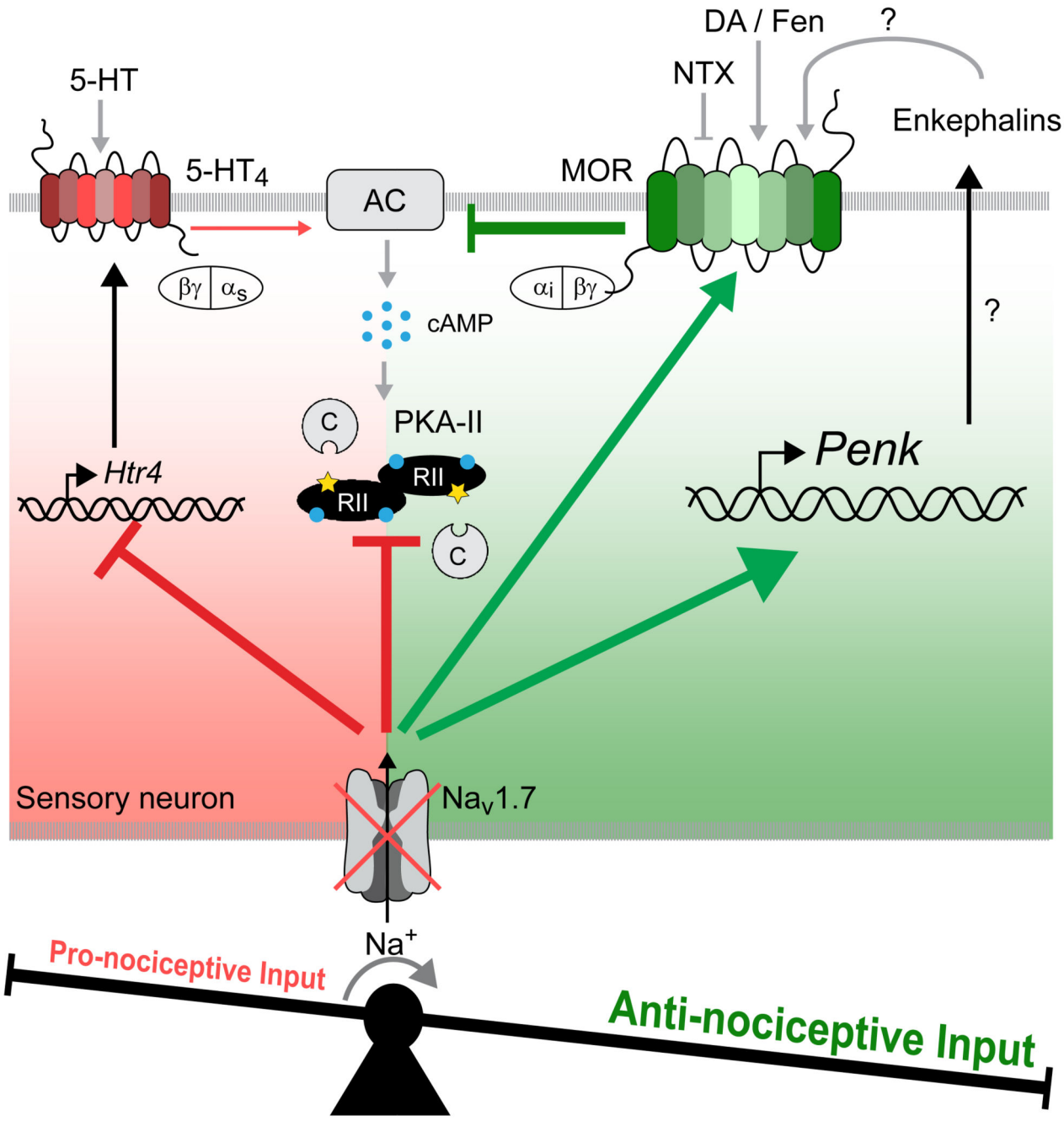

Fig. 7. Synergistic regulation of pro- and anti-nociceptive signaling in $Na_V1.7$-deficient mice.

Nav1.7-deficiency results in a reduction in 5-HT_4 receptors, due to decreased gene expression, and the RIIβ subunit (and presumably also the catalytic subunit) of PKA. Thereby, the pro-nociceptive input in sensory neurons (red) is strongly reduced. Simultaneously, the anti-nociceptive input (green) is increased due to enhanced opioid receptor activity and increased expression of the gene encoding the precursor of endogenous opioid peptides (enkephalins). This synergistic regulation shifts the balance toward anti-

nociceptive signaling and thus contributes to the pain-free phenotype in $Na_v1.7$-deficient mice.

Europe PMC Funders Author Manuscripts